# Research on Velocity Control of a Quadrotor Micro-UAV

Runnan Zou
*Department of Mechanical Engineering, University of Ottawa*
Ottawa, Canada
rzou043@uottawa.ca

***Abstract*—With surging applications of unmanned aircraft vehicle in fields of environmental protection, military and agriculture, the control of quadrotor unmanned aircraft vehicle is worth to be addressed. Aiming at finding a suitable control algorithm, two methods, proportion-feedback linearization (P-FD) and proportion-sliding mode (P-SM), are introduced into a micro-unmanned vehicle system. The control is divided into inner and outer loop. Velocity control is deployed on outer loop based on proportion control. Feedback linearization and sliding mode are applied in inner loop separately. The proposed two algorithms are tested and compared in aspect of attitude and velocity response characteristic by MATLAB/Simulink. The result shows that both methods can stabilize the attitude while P-FD performs better in tracking the required velocity.**

***Keywords—Feedback Linearization, Sliding Mode, Quadrotor UAV, Lyapunov***

## I. INTRODUCTION

With the increasing demand on man vacancy in fields of military, agriculture and remote sensing for high concealment and trafficability, unmanned aircraft vehicle (UAV) is designed and applied. With a tiny body and simple structure, characteristics of easy operate and capability of hovering, the control of quadrotor UAV has drawn worldwide researcher's attention. With six degree of freedom and only four inputs, the system of quadrotor UAV is a typical under-actuated system. The under-actuated system is easily to be disturbed which leads to the difficulty on designing a controller [1].

Many controllers are applied in UAV control [2]. For the stabilization and disturbance rejection of tracking control, PID was adapted for a quadrotor UAV [3]. However, the method of PID was still easy to be affected by external disturbance [4]. A double close-loop active disturbance rejection control was proposed by Y Zhang for tracking a target trajectory under disturbance [5]. Since the existence of nonlinear character of the system, many nonlinear control methods were applied to this field [6-7]. E. Kayacan carried out a controller based on fuzzy neural network to shifting control accuracy [8]. In [9], a nonlinear controller cooperates with trajectory prediction was proposed by B.B. Kocer. Methods contain neural network, model predictive control, PID, sliding mode and fuzzy logic control are utilized in control of UAV with outstanding performance in trajectory tracking problem [10].

In this project, a double close-loop controller is designed with two different attitude control algorithms. Feedback linearization and sliding mode are applied in attitude control of UAV. Feedback linearization transforms the nonlinear system into a local linear system with stability in order to simplify the control difficulty of system. The sliding mode control consists of a sliding surface and a law to control the system approaching the surface. Both methods can behave well in control of quadrotor UAV. With the predefined outer loop proportion controller, two controllers, proportion-feedback linearization and proportion-sliding mode, are designed and tested in MATLAB/Simulink in various initial condition, desired velocity and attitude in order to select an optimal control algorithm.

## II. MODELLING OF QUADROTOR UAV

The model of quadrotor UAV contains four rotors which is shown in Fig. 1. An inertial frame and a body fixed frame are applied in this model [6]. The UAV has six degrees of freedom consists of pitch, roll, yaw, surge, forward, left and up. The UAV is mainly affected by four force generated by four rotors and its own gravity. The thrust force is proportional to the rotor's angular speed squared. The control of rotor's angular speed can result in the manipulation of velocity and attitude of UAV.

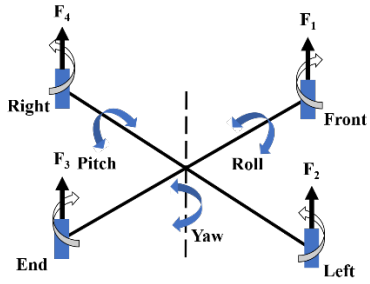


Fig. 1. Model of a quadrotor UAV

The attitude of the quadrotor UAV is presented by Euler angle $(\phi, \theta, \psi)$. The position in the inertial frame is presented by $(x, y, z)$. Since the body fixed frame is not the same as inertial frame, there is a transform matrix between these two frames as follows:

$$R = \begin{pmatrix} c_\psi c_\theta & c_\psi s_\theta s_\phi - s_\psi c_\phi & c_\psi s_\theta c_\phi + s_\psi s_\phi \\ s_\psi c_\theta & s_\psi s_\theta s_\phi + c_\psi c_\phi & s_\psi s_\theta c_\phi - c_\psi s_\phi \\ -s_\theta & c_\theta s_\phi & c_\theta c_\phi \end{pmatrix} \quad (1)$$

where $c$ denotes cosine and $s$ denotes sine.

For there are gravity and thrust force applied on the UAV, the dynamic function is:

$$\ddot{r} = g \cdot \begin{pmatrix} 0 \\ 0 \\ 1 \end{pmatrix} - R \cdot b / m \sum_{i=1}^{4} \omega_i^2 \cdot \begin{pmatrix} 0 \\ 0 \\ 1 \end{pmatrix} \quad (2)$$

where $b$ is the thrust factor and $\omega_i$ is the rotational speed of rotors. Also, for the torque applied on the UAV, the dynamic equation is built as follows:

$$I\ddot{\Omega} = -\left(\dot{\Omega} \times I\dot{\Omega}\right) - M_G + M \tag{3}$$

where $I$ is the inertia matrix, $M$ describes the torque applied on the UAV's body, $M_G$ is the gyroscopic torques which is omitted in this project. $M$ is defined as follows:

$$M = \begin{pmatrix} Lb(\omega_2^2 - \omega_4^2) \\ Lb(\omega_1^2 - \omega_3^2) \\ d(\omega_1^2 + \omega_2^2 - \omega_3^2 - \omega_4^2) \end{pmatrix} \tag{4}$$

where $b$ is the thrust factor, $d$ is the drag factor, $L$ is the length of lever. In order to simplify the dynamic euqations, the input to the system is transformed from rotor's rotational speed to a group of new inputs as follows:

$$\begin{aligned} u_1 &= b(\omega_1^2 + \omega_2^2 + \omega_3^2 + \omega_4^2) \\ u_2 &= b(\omega_2^2 - \omega_4^2) \\ u_3 &= b(\omega_1^2 - \omega_3^2) \\ u_4 &= d(\omega_1^2 + \omega_2^2 - \omega_3^2 - \omega_4^2) \end{aligned} \tag{5}$$

Therefore, the equation (2) could be transformed into the following form:

$$\begin{aligned} \ddot{x} &= -(cos\phi sin\theta cos\psi + sin\phi sin\psi)\frac{u_1}{m} \\ \ddot{y} &= -(cos\phi sin\theta sin\psi - sin\phi cos\psi)\frac{u_1}{m} \\ \ddot{z} &= g - (cos\phi cos\theta)\frac{u_1}{m} \\ \ddot{\phi} &= \dot{\theta}\dot{\psi}\left(\frac{I_y - I_z}{I_x}\right) + \frac{L}{I_x}u_2 \\ \ddot{\theta} &= \dot{\phi}\dot{\psi}\left(\frac{I_z - I_x}{I_y}\right) + \frac{L}{I_y}u_3 \\ \ddot{\psi} &= \dot{\phi}\dot{\theta}\left(\frac{I_x - I_y}{I_z}\right) + \frac{1}{I_y}u_4 \end{aligned} \tag{6}$$

The state of the system is defined as $\boldsymbol{x} = (\dot{x}, \dot{y}, \dot{z}, \phi, \theta, \psi, \dot{\phi}, \dot{\theta}, \dot{\psi})^T$. The dynamic equation is written as:

$$\dot{x} = \begin{pmatrix} -(\cos x_4 sinx_5 cosx_6 + sinx_4 sinx_6)\frac{u_1}{m} \\ -(cosx_4 sinx_5 sinx_6 - sinx_4 cosx_6)\frac{u_1}{m} \\ g - (cosx_4 cosx_5)\frac{u_1}{m} \\ x_7 \\ x_8 \\ x_9 \\ x_8 x_9\left(\frac{I_y - I_z}{I_x}\right) + \frac{L}{I_x}u_2 \\ x_7 x_9\left(\frac{I_z - I_x}{I_y}\right) + \frac{L}{I_y}u_3 \\ x_7 x_8\left(\frac{I_x - I_y}{I_z}\right) + \frac{1}{I_y}u_4 \end{pmatrix} \tag{7}$$

The dynamic equation can be divided into two parts. The first part is following:

$$\begin{pmatrix} \dot{x}_7 \\ \dot{x}_8 \\ \dot{x}_9 \end{pmatrix} = \begin{pmatrix} x_8 x_9\left(\frac{I_y - I_z}{I_x}\right) + \frac{L}{I_x}u_2 \\ x_7 x_9\left(\frac{I_z - I_x}{I_y}\right) + \frac{L}{I_y}u_3 \\ x_7 x_8\left(\frac{I_x - I_y}{I_z}\right) + \frac{1}{I_y}u_4 \end{pmatrix} \tag{8}$$

This equation is denoted as submodel $M_1$ which describes the dynamic of attitude. The second part is the submodel $M_2$ which describes the translation of UAV.

$$\begin{pmatrix} \dot{x}_1 \\ \dot{x}_2 \\ \dot{x}_3 \end{pmatrix} = \begin{pmatrix} -(\cos x_4 sinx_5 cosx_6 + sinx_4 sinx_6)\frac{u_1}{m} \\ -(cosx_4 sinx_5 sinx_6 - sinx_4 cosx_6)\frac{u_1}{m} \\ g - (cosx_4 cosx_5)\frac{u_1}{m} \end{pmatrix} \tag{9}$$

The $x_4, x_5$ and $x_6$ can be calculated based on integration of $x_7, x_8$ and $x_9$. The overall structure of dynamic model of the quadrotor UAV is depicted in Fig. 2.

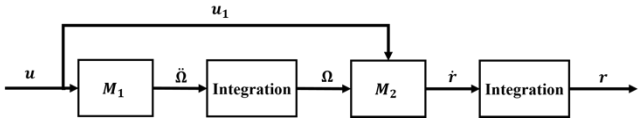


Fig. 2. Overall strucutre of dynamic model of a quadrotor UAV

## III. VEHICLE CONTROLLER DESIGN

In this project, two methods are applied in the control of UAV. Proportion-feedback linearization (P-FL) and proportion-sliding mode (P-SM) are designed separately. Both two controllers are designed in the structure of double close-loop. Controllers of the project are aiming at outputting a required velocity rather than following a trajectory. The input of the system is the required velocity. Therefore, the project is carried out based on the assumption that there exists an upper controller that generates velocity command to controllers in this project.

### *A. Proportion-feedback linearization controller*

There are two control loops exist in the controller system, velocity control loop and attitude control loop [two]. With the input of required velocity, the velocity control loop is responsible for the stabilization and generation of the input. With the input acquired from the output of velocity controller, the attitude controller is capable of controlling and stabilizing the attitude of the UAV within a relatively short time. The default command is hovering at the current position which zero in velocity and attitude angle. The model structure of controller and UAV system is shown in Fig. 3. The controller forms a nest structure.

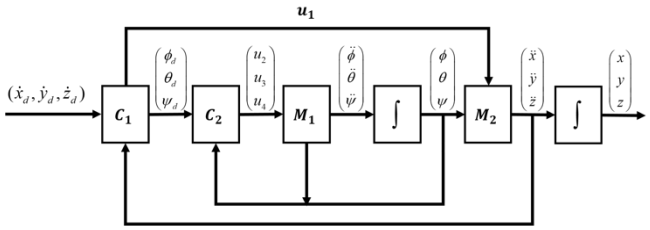


Fig. 3. Strucutre of model and controllers

The inner loop is responsible for the control and stabilization of three Euler angle. Feedback linearization is applied in attitude control:

$$\begin{aligned} u_2 &= f_2\left(x_7, x_8, x_9\right) + u_2^* \\ u_3 &= f_3\left(x_7, x_8, x_9\right) + u_3^* \\ u_4 &= f_4\left(x_7, x_8, x_9\right) + u_4^* \end{aligned} \tag{10}$$

$u_2^*$, $u_3^*$ and $u_4^*$ are new defined inputs. In order to obtain a linear system, the requirements as follows should be satisfied:

$$\begin{aligned} x_8 x_9 \left(\frac{I_y - I_z}{I_x}\right) + \frac{L}{I_x} f_2\left(x_7, x_8, x_9\right) &= K_2 \cdot x_7 \\ x_7 x_9 \left(\frac{I_z - I_x}{I_y}\right) + \frac{L}{I_y} f_3\left(x_7, x_8, x_9\right) &= K_3 \cdot x_8 \\ x_7 x_8 \left(\frac{I_x - I_y}{I_z}\right) + \frac{1}{I_y} f_4\left(x_7, x_8, x_9\right) &= K_4 \cdot x_9 \end{aligned} \tag{11}$$

where $K_2$, $K_3$ and $K_4$ are constant. The nonlinear model $M_2$ then is transformed into:

$$\begin{pmatrix} \dot{x}_7 \\ \dot{x}_8 \\ \dot{x}_9 \end{pmatrix} = \begin{pmatrix} K_2 \cdot x_7 + \dfrac{L}{I_x} u_2^* \\ K_3 \cdot x_8 + \dfrac{L}{I_y} u_3^* \\ K_4 \cdot x_9 + \dfrac{1}{I_y} u_4^* \end{pmatrix} \tag{12}$$

The controllability is verified firstly. From (12), the matrix of the linearized system is defined as follows:

$$\begin{aligned} A &= \begin{bmatrix} K_2 & 0 & 0 \\ 0 & K_3 & 0 \\ 0 & 0 & K_4 \end{bmatrix} \\ B &= \begin{bmatrix} \dfrac{L}{I_x} & 0 & 0 \\ 0 & \dfrac{L}{I_y} & 0 \\ 0 & 0 & \dfrac{1}{I_z} \end{bmatrix} \end{aligned} \tag{13}$$

The controllability matrix is then defined as follows:

$$M = \begin{bmatrix} B & AB & A^2 B \end{bmatrix} \tag{14}$$

With the parameters of the UAV and controller, $rank(M) = 3$. Therefore, the linearized submodel $M_2$ is controllable.

After the transformation, a linear system is obtained. $x_7 = 0$, $x_8 = 0$, $x_9 = 0$ is the equilibrium point of the system. With $u_2^*$=$u_3^*$=$u_{4=0}^*$, a Lyapunov function is defined as follows:

$$V\left(x_7, x_8, x_9\right) = 0.5\left(x_7^2 + x_8^2 + x_9^2\right) \tag{15}$$

$$\dot{V} = x_7 \dot{x}_7 + x_8 \dot{x}_8 + x_9 \dot{x}_9 = K_2 x_7^2 + K_3 x_8^2 + K_4 x_9^2 \tag{16}$$

Based on the calculation of derivative of $V$ in equation (14), it is shown that, $V(0) = 0$, $\dot{V} > 0$ if $K < 0$. Therefore, in the condition of $K < 0$, the designed feedback linearization attitude controller is asymptotically stable.

The equation (12) could also be written in (17). Let $x_{4d}$ be the desired $x_4$, the input $u_2^* = w_2(x_{4d} - x_4)$, $u_3^* = w_3(x_{5d} - x_5)$ and $u_6^* = w_4(x_{6d} - x_6)$ lead to a close-loop second order system in (18).

$$\begin{aligned} \ddot{x}_4 &= K_2 \dot{x}_4 + L / I_x u_2^* \\ \ddot{x}_5 &= K_3 \dot{x}_5 + L / I_y u_3^* \\ \ddot{x}_6 &= K_3 \dot{x}_6 + 1 / I_z u_4^* \end{aligned} \tag{17}$$

$$\begin{aligned} F_4(s) &= \frac{X_4(s)}{X_{4d}(s)} = \frac{w_2}{I_x / L \cdot s^2 - K_2 I_x / L \cdot s + w_2} \\ F_5(s) &= \frac{X_5(s)}{X_{5d}(s)} = \frac{w_3}{I_y / L \cdot s^2 - K_3 I_y / L \cdot s + w_3} \\ F_6(s) &= \frac{X_6(s)}{X_{6d}(s)} = \frac{w_4}{I_z \cdot s^2 - K_4 I_z \cdot s + w_3} \end{aligned} \tag{18}$$

With the predefined parameter $(K, w)$, the controller of attitude is established. The selection of $K$ should be less than zero and $\omega_i$ are calculated based on:

$$\begin{aligned} w_2 &= \left(K_2 / 2\right)^2 \cdot I_x / L \\ w_3 &= \left(K_3 / 2\right)^2 \cdot I_y / L \\ w_4 &= \left(K_4 / 2\right)^2 \cdot I_z \end{aligned} \tag{19}$$

The inner loop is able to response in a short time. The outer loop generates the desired x4dx5dx6d and the attitude loop delivers x4x5x6 to M2 in s short time. The submodel $M_2$ in equation (9) is transform into the form of equation (18).

$$\begin{aligned} \dot{x}_1 &= \tilde{u}_1 = f_1(x_{4d}, x_{5d}, x_{6d}, u_1) \\ \dot{x}_2 &= \tilde{u}_2 = f_2(x_{4d}, x_{5d}, x_{6d}, u_1) \\ \dot{x}_3 &= \tilde{u}_3 = f_3(x_{4d}, x_{5d}, x_{6d}, u_1) \end{aligned} \tag{20}$$

where $\tilde{u}$ is the artificial input. Since the model $M_2$ is simple, proportional control is applied in velocity controller:

$$\begin{aligned}\tilde{u}_1 &= k_1(x_{1d} - x_1)\\ \tilde{u}_2 &= k_2(x_{2d} - x_2)\\ \tilde{u}_3 &= k_3(x_{3d} - x_3)\end{aligned} \tag{21}$$

where $k_1$, $k_2$ and $k_3$ are the proportional factors respectively. $x_{1d}$, $x_{2d}$ and $x_{3d}$ are the demand velocity input of the system. It is obvious the desired velocity can be achieved without any yaw rotation. Therefore, $x_{6d} = 0$. The equation (20) is simplified as:

$$\begin{aligned}\tilde{u}_1 &= -\cos x_{4d} sinx_{5d} cosx_{6d} \frac{u_1}{m}\\ \tilde{u}_2 &= sinx_{4d} cosx_{6d} \frac{u_1}{m}\\ \tilde{u}_3 &= g - (cosx_{4d} cosx_{5d}) \frac{u_1}{m}\end{aligned} \tag{22}$$

Then by applying the substitution:

$$\begin{aligned}\alpha &= sinx_{4d}\\ \cos x_{4d} &= \sqrt{1-\alpha^2}\\ \beta &= sinx_{5d}\\ \cos x_{5d} &= \sqrt{1-\beta^2}\end{aligned} \tag{23}$$

The solution is obtained:

$$\begin{aligned}\beta &= \pm\left[\left(\frac{g-\tilde{u}_3}{\tilde{u}_1}\right)^2 + 1\right]^{-\frac{1}{2}}\\ u_1 &= \pm m \cdot \sqrt{\frac{\tilde{u}_1^2}{\beta^2} + \tilde{u}_2^2}\\ \alpha &= \tilde{u}_2 \cdot \frac{m}{u_1}\end{aligned} \tag{24}$$

From equation (5), $u_1$ is always positive. Therefore, $u_1 = m\sqrt{\frac{\tilde{u}_1^2}{\beta^2} + \tilde{u}_2^2}$. $x_{4d}$ and $x_{5d}$ are also unique in the internal $[-\frac{\pi}{2}, \frac{\pi}{2}]$, therefore, $x_{4d} = \arcsin(\alpha)$ and $x_{5d} = \arcsin(\beta)$. However, the sign of $x_{5d}$ is unsettling. Considering the equation:

$$\tilde{u}_1 = -\cos x_{4d} sinx_{5d} cosx_{6d} \frac{u_1}{m} \tag{25}$$

It could be drawn that, $cosx_{4d}$ is always positive, the $x_{5d}$ is positive if $u_1$ is negative and vice versa. If $\widetilde{u_1} = 0$, then $x_{5d} = 0, u_1 = m\sqrt{\frac{\tilde{u}_1^2}{\beta^2} + \tilde{u}_2^2}, x_{4d} = \arcsin(\alpha)$.

Then the controller of P-FL is established. Two controller generates four control order to the system. These four control variables are then utilized to calculated input rotational speed of the UAV. This controller is capable of generating output in a relatively short time.

*B. Proportion-sliding mode controller*

The proportion-sliding mode controller is designed by me based on the fixture of proportional control and sliding mode control in order to compare the output performance between P-FL and P-SM. The P-SM contains the same structure as P-FL that there is a double close-loop structure and proportional control is deployed in the outer loop. In the P-SM, sliding mode control is applied in attitude control. In the control of attitude, sliding mode is introduced as the attitude controller. Firstly, the sliding surface function is defined as follows:

$$S = \dot{e} + K_p e \tag{26}$$

where $K_p$ is the proportional factor, $e$ is the tracking error. As the dynamic function of submodel $M_2$ is (8) and the tracking error is defined as $e_1 = x_4 - x_{4d}$, $e_2 = x_5 - x_{5d}$ and $e_3 = x_6 - x_{6d}$, the sliding mode surface is:

$$\begin{aligned}S_1 &= \dot{x}_4 - \dot{x}_{4d} + K_{p1}(x_4 - x_{4d})\\ S_2 &= \dot{x}_5 - \dot{x}_{5d} + K_{p2}(x_5 - x_{5d})\\ S_3 &= \dot{x}_6 - \dot{x}_{6d} + K_{p3}(x_6 - x_{6d})\end{aligned} \tag{27}$$

Choosing the following as the exponential reaching law:

$$\dot{S} = -M \cdot sat(y) \tag{28}$$

where $M$ is a positive constant and $sat()$ is a saturation function defined as follows:

$$sat(y) = \begin{cases} y & |y| \le 1 \\ sgn(y) & |y| > 1 \end{cases} \tag{29}$$

where $y = S/\lambda$, $\lambda$ denotes the thickness of boundary layer, $sgn()$ presents a sign function.

The control inputs are designed as follows:

$$\begin{aligned}u_2 &= \frac{I_x}{L}\left(-x_8 x_9\left(\frac{I_y - I_z}{I_x}\right) + \dot{x}_{7d} - K_{p1}(x_7 - x_{7d}) - Msat(y)\right)\\ u_3 &= \frac{I_y}{L}\left(-x_7 x_9\left(\frac{I_z - I_x}{I_y}\right) + \dot{x}_{8d} - K_{p2}(x_8 - x_{8d}) - Msat(y)\right)\\ u_4 &= \frac{1}{L}\left(-x_8 x_7\left(\frac{I_x - I_y}{I_z}\right) + \dot{x}_{9d} - K_{p3}(x_9 - x_{9d}) - Msat(y)\right)\end{aligned} \tag{30}$$

It is necessary to verify the stability of the new attitude controller. Considering the Lyapunov function as follows:

$$V = \frac{1}{2} S^2 \tag{31}$$

The derivative of the Lyapunov function is shown as follows:

$$\begin{aligned}\dot{V} &= S\dot{S}\\ &= S(-Msat(y))\\ &= -Msat(S/\lambda) \cdot S \le 0\end{aligned} \tag{32}$$

Therefore, the attitude controller is asymptotically stable. The main advantage of sliding mode control is its robustness under the condition of environmental disturbance. With the

designed saturation function, the frequent oscillation is prevented.

## IV. SIMULATION

Several simulations are carried out in this section to compare the effectiveness of two controller. The parameters are set as the same in two groups of simulation as shown in Table I. The proportional factor for the P-FL is $k_1 = k_2 = k_3 = 5$ while in P-SM $k_1 = k_2 = k_3 = 0.5$. The inner loop parameter of P-FL is $K_2 = K_3 = K_4 = -80, w_2 = w_3 = 38, w_4 = 14$. The parameter of inner loo p parameter of P-SM is $M = 25, K_{p1} = 5.5, K_{p2} = 5.5, K_{p3} = 8.5$.

TABLE I. PARAMETERS OF THE QUADROTOR UAV

| Parameters | Value | Unit |
|---|---|---|
| g | 9.81 | m/s$^2$ |
| m | 0.5 | kg |
| L | 0.2 | m |
| $I_x$=$I_y$ | 4.85×10-3 | kgm$^2$ |
| $I_z$ | 8.81×10-3 | kgm$^2$ |
| b | 2.92×10-6 | kgm$^2$ |
| d | 1.12 ×10-7 | kgm$^2$ |

In the first simulation, an initial condition of $\Omega^T = (\phi = 0.523, \theta = -0.349, \psi = 0.174)$ and $\dot{x} = 0, \dot{y} = 0, \dot{z} = 0$ are given. The control goal is to stabilize a hover position. Therefore, $x_{1d} = 0\, x_{2d} = 0\, x_{3d} = 0$. Fig. 4 (a) and (b) present the velocity plot of the quadrotor UAV by P-Fl and P-SM. Fig. 5 (a) and (b) show the angles variation plot of time for four quadrotors. From Fig. 4, it could be seen that P-FL comes to stability within 0.7 seconds while it costs 10 seconds for P-SM. Compared with P-SM, the P-FL has less overshoot and the time goes to stability. In the aspect of attitude, both methods perform well, three angles go to zero in a short time.

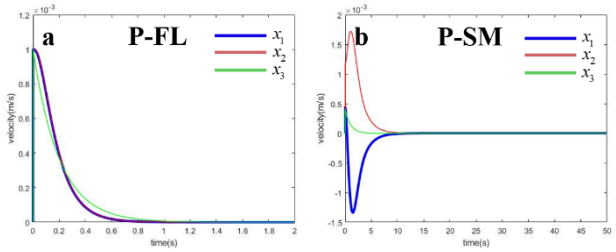


Fig. 4. Velocity behavior of two algorithms

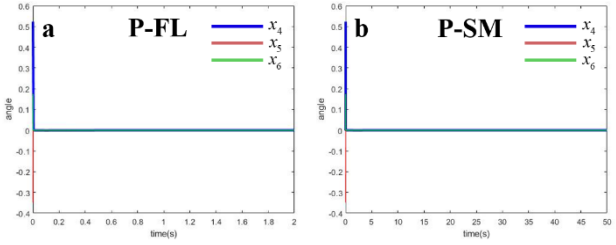


Fig. 5. Attitude behavior of two algorithms

In the second simulation, the initial condition is $\dot{x} = 0.8, \dot{y} = 0, \dot{z} = 0$ and $\phi = 0, \theta = 0, \psi = 0$. The control goal is also staying at the hovering position that $x_{1d} = 0\, x_{2d} = 0\, x_{3d} = 0$. The angular plot of the UAV is shown in Fig. 7 (a) and (b). The velocity plot of the UAV is shown in Fig. 8 (a) and (b). in the aspect of velocity, in simulation of P-FL, the velocity goes to zero immediately while the velocity of P-SM converges to 0 in 8 seconds with some oscillations. It costs more time for P-SM's controller to hover at the position. In Fig. 7, with a little overshoot, the angle of P-FL converges to zero in 0.8 seconds while great overshoot has happened on P-SM's controller, the stable time is 10 seconds. In the simulation of P-SM, the proportional factor has been adjusted several times for balancing the overshoot and stable time.

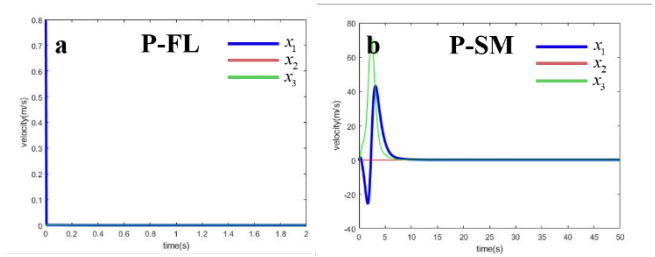


Fig. 6. Velocity behavior of two algorithms

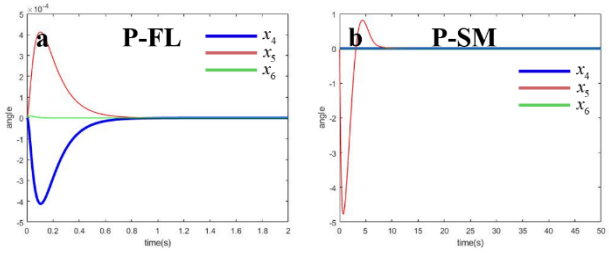


Fig. 7. Attitude behavior of two algorithms

In the third simulation, the initial condition is $\dot{x} = 0, \dot{y} = 0, \dot{z} = 0$ and $\phi = 0, \theta = 0, \psi = 0$. The desired velocity is $\dot{x} = 0.5, \dot{y} = 0.5, \dot{z} = 0.5$. The attitude angle and velocity of UAV of are shown in Fig. 9 (a) (b) and Fig. 10 (a) (b), respectively. From Fig. 8 (a), the trajectory of velocity is depicted. The velocity converges to the desired value in 0.8 seconds with no overshoot existed. However, in Fig. 8 (b), great overshoot has happened with settling time of 5 seconds. Compared with P-FL, either overshoot or long stable time exists. In Fig. 9, P-FL stables the system with relatively small overshoot and short settling time compared with P-SM.

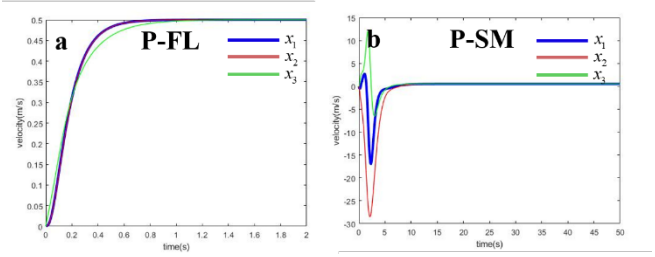


Fig. 8. Velocity behavior of two algorithms

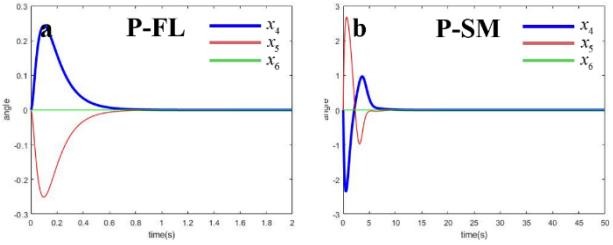


Fig. 9. Attitude behavior of two algorithms

In these simulations, each parameter has been tuned carefully. Therefore, the performance of two algorithms reflects their property towards the system of quadrotor UAV system. Compared with P-SM, the controller of P-FL can

quickly stable the system with relatively small overshoot. Both attitude and velocity converge to the desired value. Therefore, P-FL outperforms P-SM in control of velocity and attitude of quadrotor UAV.

## V. CONCLUSION

In this project and report, a model of quadrotor UAV is introduced and established. In order to research on the characteristic for controllers of proportion-feedback linearization and proportion-sliding mode, two controllers are well designed and built in MATLAB/Simulink. Two controllers' performance are generated by implementing three different simulations. From the result obtained on velocity and attitude, P-FL outperforms P-SM in aspect of behavior on attitude and velocity.

Moreover, there still some improvements could be exerted on two controllers. For both of them, the proportion part could be improved to proportion-integration control to overcome the overshoot. The verification of two controller could be carried out in more different initial conditions and desired destinations for a thorough test.

## REFERENCES


[1] Voos H. Nonlinear control of a quadrotor micro-UAV using feedback-linearization[C]. 2009 IEEE International Conference on Mechatronics. IEEE, 2009: 1-6.

[2] Voos H. Nonlinear and neural network-based control of a small four-rotor aerial robot[C]. 2007 IEEE/ASME international conference on advanced intelligent mechatronics. IEEE, 2007: 1-6.

[3] Bolandi H, Rezaei M, Mohsenipour R, et al. Attitude control of a quadrotor with optimized PID controller[J]. 2013.

[4] Li J, Guo H, Zhang H, et al. Double-loop structure integral sliding mode control for UUV trajectory tracking[J]. IEEE Access, 2019, 7: 101620-101632.

[5] Zhang Y, Chen Z, Zhang X, et al. A novel control scheme for quadrotor UAV based upon active disturbance rejection control[J]. Aerospace Science and Technology, 2018, 79: 601-609.

[6] Castillo P, Dzul A, Lozano R. Real-time stabilization and tracking of a four-rotor mini rotorcraft[J]. IEEE Transactions on control systems technology, 2004, 12(4): 510-516.

[7] Choi Y C, Ahn H S. Nonlinear control of quadrotor for point tracking: Actual implementation and experimental tests[J]. IEEE/ASME transactions on mechatronics, 2014, 20(3): 1179-1192.

[8] Kayacan E, Maslim R. Type-2 fuzzy logic trajectory tracking control of quadrotor VTOL aircraft with elliptic membership functions[J]. IEEE/ASME Transactions on Mechatronics, 2016, 22(1): 339-348.

[9] Kocer B B, Tjahjowidodo T, Seet G G L. Centralized predictive ceiling interaction control of quadrotor VTOL UAV[J]. Aerospace Science and Technology, 2018, 76: 455-465.

[10] Yin H, Wang Q, Sun C. Position and attitude tracking control for a quadrotor UAV via double-loop controller[C]. 2017 29th Chinese Control And Decision Conference (CCDC). IEEE, 2017: 5358-5363.